

APMP Key Comparison Report of air kerma for  $^{137}\text{Cs}$   
(APMP.RI(I)-K5)

I. J. Kim<sup>a</sup>, C-Y. Yi<sup>a</sup>, N. C. Díaz<sup>b</sup>, S.-W. Wang<sup>c</sup>, Y-C. Lin<sup>c</sup>,  
Y. Zhang<sup>d</sup>, D. Li<sup>d</sup>, T. Kurosawa<sup>e</sup>, N. Saito<sup>e</sup>,

<sup>a</sup>*Korea Research Institute of Standards and Science, Daejeon, Korea*

<sup>b</sup>*Laboratorio de Metrología de Radiaciones Ionizantes (Spanish National Metrology Laboratory for Ionising Radiation)*

<sup>c</sup>*Institute of Nuclear Energy Research, Longtan, Taiwan (R.O.C.)*

<sup>d</sup>*National Institute of Metrology, Beijing, China*

<sup>e</sup>*National Metrology Institute of Japan, Tsukuba, Japan*

## Abstract

The APMP/TCRI Dosimetry Working Group performed the APMP.RI(I)-K5 key comparison of the air kerma for  $^{137}\text{Cs}$  in 2014. Five national metrology institutes (NMIs) took part in the comparison. Two commercial ionization chambers were used as transfer instruments and circulated among the participants. The results showed that the maximum difference between the participants and the Bureau International des Poids et Mesures, evaluated using the comparison data of the linking laboratories of the Korea Research Institute of Standards and Science and the National Metrology Institute of Japan, was less than 0.5% within the expanded uncertainty. This comparison supports the equivalence of the calibration capabilities of the participating laboratories. The results predate the publication of ICRU report 90, therefore, the revision of the data reflecting the effects of the ICRU report 90 on the degrees of equivalences of the participant laboratories is presented in Appendix C.

## 1. Introduction

A key comparison of the high intensity  $^{137}\text{Cs}$  gamma-ray air kerma measurement was agreed to be undertaken in the Technical Committee for Ionizing Radiation (TCRI) of the Asia Pacific Metrology Programme (APMP) in 2011. The objective of this key comparison study was to establish the degrees of equivalence ( $D_i$ ) of national standards and to support the calibration and measurement capabilities (CMCs) of ionization chamber calibrations for radiation protection.

A total of five laboratories participated in the comparison in 2014, where the Korea Research Institute of Standards and Science (KRISS) was the pilot laboratory. The comparison was undertaken indirectly using two ionization chambers as the transfer instruments. The transfer ionization chambers were circulated using a star-shaped circulation scheme between the KRISS and the participating laboratories. The KRISS, as a pilot laboratory, took responsibility for supervising transportation of the transfer

ionization chambers to and from the participating laboratories and evaluating the results submitted by the laboratories.

The degree of equivalence of the participating laboratories was derived from the calibration coefficients of the transfer ionization chambers reported by the participating laboratories. The results were linked to the key comparison reference value (KCRV) via the results of two linking laboratories (LINK) of the KRISS and the National Metrology Institute of Japan (NMIJ).

The five participating laboratories were: 1) Centro de Investigaciones Energéticas, Medioambientales y Tecnológicas (CIEMAT), Kingdom of Spain; 2) Institute of Nuclear Energy Research (INER), Taiwan; 3) National Institute of Metrology (NIM), China; 4) National Metrology Institute of Japan (NMIJ), Japan; 5) Korea Research Institute of Standards and Science (KRISS), Republic of Korea. The information of the five participating laboratories and their contact persons for this APMP.RI(I)-K5 comparison study is as listed in Table 1.

Table 1. Participating laboratories and contact persons

Institute	Economy	Contact person (e-mail)
CIEMAT	Spain	Néstor Cornejo Díaz ( <a href="mailto:nestorarmando.cornejo@ciemat.es">nestorarmando.cornejo@ciemat.es</a> )
INER	Taiwan	Yi-Chun Lin ( <a href="mailto:jasmyna@iner.gov.tw">jasmyna@iner.gov.tw</a> )
NIM	China	Yanli Zhang ( <a href="mailto:zhangyl@nim.ac.cn">zhangyl@nim.ac.cn</a> ), Dehong Li ( <a href="mailto:lidh@nim.ac.cn">lidh@nim.ac.cn</a> )
NMIJ	Japan	Tadahiro Kurosawa ( <a href="mailto:tadahiro-kurosawa@aist.go.jp">tadahiro-kurosawa@aist.go.jp</a> ), Norio Saito ( <a href="mailto:norio.saito@aist.go.jp">norio.saito@aist.go.jp</a> )
KRISS	Korea	Chul-Young Yi ( <a href="mailto:cyyi@kriss.re.kr">cyyi@kriss.re.kr</a> )

## 2. Procedure

### 2.1 Transfer instruments

Two ionization chambers were used as the transfer instruments for this comparison study. An Exradin A3 (S/N 110) and a PTW TN23331 (S/N 0833) chamber were chosen to measure the relatively high intensity  $^{137}\text{Cs}$  beams. The volumes of the chambers were 3.6 and 1 cm<sup>3</sup>, respectively, which was large enough to produce sufficiently large ionization currents whilst minimizing ion recombination and beam non-uniformity effects. The transfer ionization chambers were circulated without an electrometer and each participating laboratory used its own measuring system. The technical data of the transfer ionization chambers were as shown in table 2.

The Exradin A3 (S/N 110) was as shown in figure 1. The outer diameter and stem length were 23.5 mm and 28.5 cm, respectively. No build-up cap was provided since the ionization chamber had a 2.5 mm thick wall composed of the C-552 air equivalent plastic. A bias voltage cable was connected to the chamber via a banana plug, and the signal cable was connected via a BNC connector.

Table 2. Technical data of the transfer ionization chambers

Model	Serial number	Nominal volume	Cavity radius	Bias voltage <sup>a)</sup>	Cable connection
Exradin A3	110	3.6 cm <sup>3</sup>	0.95 cm	- 300 V	BNC & banana plug
PTW TN23331	0833	1 cm <sup>3</sup>	0.345 cm	- 400 V	Triaxial; adaptor for BNC & banana plug

<sup>a)</sup> Negative bias voltage was supplied to the chamber wall with respect to the central electrode which was at virtual ground.



Fig. 1. A photograph of the Exradin A3 ionization chamber (S/N 110).

The PTW TN23331 (S/N 0833) was as shown in figure 2. The stem length was 32.7 cm. A build-up cap of 3 mm thick poly methyl methacrylate (PMMA) was provided because the chamber had thin layers of walls composed of PMMA (65 mg/cm<sup>2</sup> thick) and graphite (54 mg/cm<sup>2</sup> thick). The outer diameter of the chamber with the build-up cap on was 15.0 mm. A cable converter from a tri-axial to a BNC/banana-plug set was also provided so that the participating laboratories could connect their measurement system to the chamber if needed.



Fig. 2. A photograph of the PTW TN23331 ionization chamber (S/N 0833).

## 2.2 Comparison structure and schedule

Two transfer ionization chambers were circulated using a star-shaped circulation scheme between the KRISS and the participating laboratories. The KRISS performed the chamber repeatability test every time when the chambers were sent to the participating laboratories in order to prevent errors due to instability issues.

The proposed schedule of the circulation was as shown in table 3. The circulation was scheduled to commence on 03-Feb-2014 and to be completed on 20-Oct-2014. In order to avoid successive delays in the comparison schedule, the transfer chambers didn't stay at the participants' laboratories for longer than two weeks. Because of the rainy season in the East Asian region, there was a break from June to August.

Table 3. Proposed schedule of the circulation of the transfer chambers for the comparison study APMP.RI(I)-K5.

Participant	Sent to the participant	Measurement at the participating laboratory	Returned from the participant
NMIJ	03-Feb-2014	17-Feb-2014 to 28-Feb-2014	03-Mar-2014
INER	24-Mar-2014	07-Apr-2014 to 18-Apr-2014	21-Apr-2014
CIEMAT	12-May-2014	26-May-2014 to 06-Jun-2014	09-Jun-2014
NIM	22-Sep-2014	06-Oct-2014 to 17-Oct-2014	20-Oct-2014

## 2.3. The linking of regional comparisons to international comparisons for eligible institutes

Following the decision of the Consultative Committee for Ionizing Radiation (CCRI), the Bureau International des Poids et Mesures (BIPM) determination of the dosimetric quantity, here  $K_{\text{BIPM}}$ , was taken as the key comparison reference value (KCRV) [1]. The ratio of the calibration coefficient reported by the  $i$ -th participating laboratory to the KCRV,  $R_i$ , was determined as [2]:

$$R_i = \frac{N_{K,i}}{N_{K,\text{LINK}}} R_{\text{LINK,BIPM}} \quad (1)$$

where  $N_{K,i}$  (or  $N_{K,\text{LINK}}$ ) is the air kerma calibration coefficient reported by the  $i$ -th participating laboratory (or the LINK);  $R_{\text{LINK,BIPM}}$  represents the result of the LINK in the BIPM international comparison BIPM.RI(I)-K5. In this study, the KRISS and the NMIJ played the role of the linking laboratories. They made direct comparisons of their standards for air kerma with the BIPM in 2010 [3] and 2012 [4], respectively.  $R_{\text{LINK,BIPM}}$  of each LINK was calculated as [2-4]:

$$R_{\text{LINK,BIPM}} = \frac{K_{\text{LINK}}^{\text{inter}}}{K_{\text{BIPM}}} \quad (2)$$

where  $K_{\text{LINK}}^{\text{inter}}$  is the air kerma rate reported by the LINK in the BIPM.RI(I)-K5.  $R_{\text{LINK,BIPM}}$  of the LINKs and the related uncertainty were as shown in table 4.

In this case (with two linking laboratories), equation (1) gives rise to two values of  $R_i$  for each participating laboratory  $i = 1$  to  $(n-2)$ , not acting as a linking laboratory. Denoting these values as  $R_{i,KRISS}$  and  $R_{i,NMIJ}$ , the  $R_i$  values for these laboratories were calculated as [2]:

$$R_i = \frac{R_{i,KRISS} + R_{i,NMIJ}}{2} \quad (3)$$

Table 4.  $R_{LINK,BIPM}$  of the LINKs in the key comparison study of the air kerma for  $^{137}\text{Cs}$  gamma-rays, BIPM.RI(I)-K5

	$R_{LINK,BIPM}$	Relative standard uncertainties				Remarks
		$u_{R,LINK,BIPM}$	$u_{K,LINK,stat}^{a)}$	$u_{K,LINK,non-stat}^{b)}$	$u_{BIPM}$	
KRISS	0.998 6	0.22	0.05	0.21	0.19	2010 [3]
NMIJ	0.997 7	0.26	0.16	0.20	0.19	2012 [4]

a)  $u_{K,LINK,stat}$  represents the type A relative standard uncertainty estimated by statistical methods.

b)  $u_{K,LINK,non-stat}$  represents the type B relative standard uncertainty by other means.

The standard uncertainty of  $R_i$  was estimated as [2]:

$$u_{R,i}^2 = [u_i^2 + u_{BIPM}^2 - \sum_j f_j^2 (u_{i,j}^2 + u_{BIPM,j}^2)] + u_{tr}^2 + u_{LINK}^2 \quad (4)$$

where  $u_i$  is the combined standard uncertainty of the calibration coefficient reported by the  $i$ -th participating laboratory (not including the components arising from the transfer chamber);  $u_{BIPM}$  is the combined standard uncertainty of the BIPM's air kerma rate standard ( $K_{BIPM}$ ) as described in the BIPM.RI(I)-K5;  $u_{tr}$  is the uncertainty arising from the transfer chamber; and  $u_{LINK}$  represents the uncertainty arising from the linking mechanism. The summation contains those components  $f_j u_{i,j}$  and  $f_j u_{BIPM,j}$  which were correlated between laboratory  $i$  and the BIPM, with correlation factor  $f_j$ .

There are two approaches available to estimate  $u_{tr}$  [2]. In the first approach, for one transfer chamber,  $u_{tr}$  is calculated as the adjusted standard deviation of the  $m$  repeat calibrations  $N_{K,pilot,j}$  ( $j=1$  to  $m$ ) made by the pilot laboratory for testing the repeatability of the transfer chamber :

$$u_{tr}^2 = \frac{1}{(m-1.4)} \sum_j^m (N_{K,pilot,j} - N_{K,pilot})^2 \quad (5)$$

where  $N_{K,pilot}$  is the mean of the  $N_{K,pilot,j}$  from all repeat calibrations.

In the second approach, for multiple transfer chambers,  $u_{tr}$  could be obtained as:

$$u_{tr}^2 = \frac{1}{p(p-1.4)} \sum_j^p (R_{i,j} - R_i)^2 \quad (6)$$

where  $p$  is the number of transfer chambers used in the study and  $R_{i,j}$  represents the  $i$ -th participating laboratory's ratio  $R$  obtained with the  $j$ -th transfer chamber.

$u_{\text{LINK}}$  could also be estimated by two different approaches [2]. In the first approach,  $u_{\text{LINK}}$  is given as:

$$u_{\text{LINK}}^2 = \left( \sum_{k=1}^q \frac{1}{u_{\text{LINK},k}^2} \right)^{-1} \quad (7)$$

$$u_{\text{LINK},k}^2 = 2u_{K,\text{LINK},k,\text{stat}}^2 + u_{I,\text{LINK},k}^2 \quad (8)$$

where  $q$  is the number of LINKs involved in the comparison study;  $u_{K,\text{LINK},k,\text{stat}}$  is the type A standard uncertainty of  $K_{\text{LINK},k}$  reported by the  $k$ -th LINK in the BIPM.RI(I)-K5 key comparison, and  $u_{I,\text{LINK},k}$  is the combined standard uncertainty of the ionization current  $I_{\text{LINK},k}$  measured by the  $k$ -th LINK.

If equation (5) is used for  $u_{\text{tr}}$  then for  $k = \text{KRIS}$  (pilot laboratory) the following equation shall be used:

$$u_{\text{LINK},k}^2 = u_{K,\text{LINK},k,\text{stat}}^2 + u_{I,\text{LINK},k,\text{non-stat}}^2 \quad (9)$$

where  $u_{I,\text{LINK},k,\text{non-stat}}$  represents the non-statistical component of the  $I_{\text{LINK},k}$ .

In the second approach,  $u_{\text{LINK}}$  is calculated as:

$$u_{\text{LINK}}^2 = \frac{1}{q(q-1.4)} \sum_k^q (R_{i,k} - R_i)^2 \quad (10)$$

where  $R_{i,k}$  is the  $i$ -th participating laboratory's ratio  $R$  obtained against the  $k$ -th LINK.

The larger of the  $u_{\text{LINK}}$  values obtained from equations (7) and (10) is the best estimate of  $u_{\text{LINK}}$  to be used in equation (4).

### 2.3 Reference conditions, measurement procedure and report of results

For acclimatization of the transfer chambers, the participants were asked to place the chambers in the laboratories at least 12 hours before the measurements. The electrometers and high voltage supplies were required to be warmed up for at least 2 hours and allowed to stabilize for more than one hour after the high voltage was applied to the chambers.

The reference point of the transfer chambers was on the chamber axis at the center of the cavity volume. The presumed center of the chambers was marked on each chamber surface for visual aid. The chambers were positioned with the stem perpendicular to the beam axis, and the source-to-chamber distance was 1 m. The ionization current of the PTW TN23331 chamber was measured with the provided build-up cap attached. For the Exradin A3, no build-up cap was needed since it had a thick wall.

The participants were asked to measure the background current before and after the measurements of the ionizing current produced by the  $^{137}\text{Cs}$  gamma-rays and then to obtain the net ionization current by subtracting the average background current. The measurements were repeated at least ten times to get a set of measurement for each chamber. The temperature, the air pressure and the humidity were also

requested to be monitored during the measurements for the correction of the environmental effects. The reference environmental conditions were at 293.15 K, 101.325 kPa and 50 % relative humidity. The participating laboratories were not requested to apply the ion recombination correction. (Recombination effect was less than 0.2 % for the Exradin A3 chamber at the KIRSS.)

The air kerma calibration coefficient of the chambers was determined at the participating laboratories as

$$N_K = (K/I) \prod_i k_i \quad (11)$$

where  $N_K$  is the air kerma calibration coefficient given in units of Gy/C,  $K$  is the air kerma rate in Gy/s,  $I$  is the net ionization current in A, and  $k_i$  is the  $i$ -th correction factor.  $I$  was measured at the negative polarity only, as can be seen in Table 2, and no polarity correction was needed. Uncertainties were evaluated in accordance to the ISO guidance [5].

An Excel spreadsheet template for reporting the measurement results was sent to participating laboratories. The following information was requested to be reported by each participating laboratory:

- a. Cs-137 source
  - Nominal activity
  - Source dimension, capsule dimension & material (if available)
- b. Electrometer
  - Manufacturer & model
  - Operation mode (charge or current)
  - Traceability
- c. Pre-calibrated standard chamber used in measurement
  - Manufacturer, model & serial number
  - Traceability
  - Calibration date
  - Calibration distance
  - Air kerma rate during calibration at the laboratory of traceability
  - Calibration coefficient
  - Uncertainty of the calibration coefficient ( $k = 1$ )
- d. Measurement procedure
  - Chamber climatization time at participant's site
  - Date and time when chamber bias voltage was applied (yyyy-mm-dd hh:mm:ss)
  - Duration of pre-irradiation
  - Start date and time of measurement (yyyy-mm-dd hh:mm:ss)
  - Finish date and time of measurement (yyyy-mm-dd hh:mm:ss)
  - Number of repeat measurements

- e. Measurement results
- Temperature range during measurement
  - Atmospheric pressure range during measurement
  - Relative humidity range during measurement
  - Calibration distance (source to reference point)
  - Beam cross-section on the reference plane
  - Air kerma rate at the reference point
  - Background current
  - Net ionization current (background current subtracted)
  - Calibration coefficient (Gy/C)
- f. Uncertainties budget in % ( $k = 1$ )

### 3. Results

Results of the repeatability test of the transfer chambers performed at the pilot laboratory were as shown in table 5 and figure 3.

Table 5. Results of the chamber repeatability test conducted at the pilot laboratory

	Exradin A3 (S/N 110)		PTW TN23331 (S/N 0833)		Remarks
	Mean, Gy/ $\mu$ C	RSD	Mean, Gy/ $\mu$ C	RSD	
23-Jan-2014	8.569	0.007 %	28.54	0.006 %	Before NMIJ
24-Mar-2014	8.570	0.006 %	28.37	0.002 %	After NMIJ
08-May-2014	8.571	0.009 %	28.07	0.004 %	After INER
18-Jun-2014	8.571	0.005 %	28.25	0.002 %	After CIEMAT
22-Aug-2014	8.572	0.002 %	28.20	0.003 %	Before NIM
22-Jan-2015	8.573	0.001 %	28.13	0.007 %	After NIM

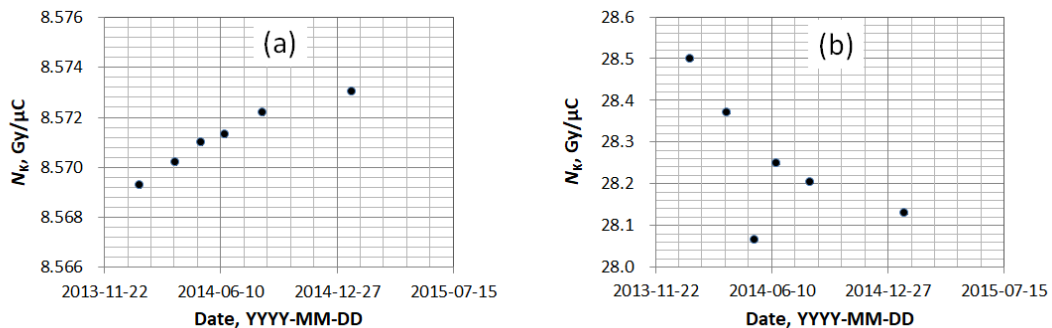


Fig. 3. Air kerma calibration coefficients of the Exradin A3 (S/N 110) (a) and the PTW TN23331 (S/N 0833) (b) measured at the KRISS to check the stability of the chambers during the period of the comparison study.

The PTW TN23331 (S/N 0833) chamber showed a drastic change over time. The change over the comparison period was up to 1.3 %. A sharp drop was observed on May 8 after the chamber came back from the INER as shown in figure 3. In addition, the ionization current of the chamber did not stabilize for several hours after the start of irradiation, which is discussed in Appendix A. CCRI(I)/17-09 [2] requests a correction for the response of transfer chambers when a statistically significant jump or drift is found. However, this kind of chamber instability was very unusual. Therefore, it was decided to exclude the results obtained with this chamber from the evaluation of the degree of equivalence of the participating laboratories.

For the Exradin A3 (S/N 110) chamber, the chamber response increased slightly over time. However, correction for this chamber response was not made since the change was only 0.05 %.  $u_{tr}$  of this chamber was estimated at 0.02 % according to equation (5).

The experimental conditions during measurements and the air kerma calibration coefficients reported by the participating laboratories were as shown in tables 6 and 7, respectively. Uncertainties in table 7 are regarded as global across those two chambers. The detailed uncertainty budgets for all the participating laboratories are given in Appendix B.

Table 6. Experimental conditions during calibration measurements.

Participant	Air kerma rate, mGy/s	Beam size <sup>a)</sup>	Temperature, °C	Pressure, kPa	R.H. <sup>b)</sup> , %
KRISS	1.06	11.6 cm, dia.	22.3 - 23.3	100.7 - 102.2	39 - 45
NMIJ	0.39	22 cm, dia.	22.3 - 22.5	101.1 - 102.1	17 - 21
INER	0.35	(10×10) cm <sup>2</sup>	21.6 - 23.0	98.6 - 98.8	41 - 44
CIEMAT	0.70	14.6 cm, dia.	20.2 - 20.3	93.90-93.92	36.9-37.0
NIM	0.039	15 cm, dia.	19.5 - 24.5	100.5 - 102.5	30 - 60

<sup>a)</sup> Beam cross-section on the reference plane of the measurement

<sup>b)</sup> R.H. stands for relative humidity

Table 7. The air kerma calibration coefficients,  $N_K$ , reported by the participating laboratories

Participant	$N_K$ ( $10^7$ Gy C <sup>-1</sup> )		Relative standard uncertainty $u_r(N_K)$ (%)
	A3 (S/N 110)	TN23331 (S/N 0833)	
KRISS	0.856 9	2.853 5	0.21
NMIJ	0.860 9	2.856 0	0.24
INER	0.856 5	2.816 0	0.30
CIEMAT	0.864 1	2.842 0	0.78
NIM	0.861 6	2.845 0	0.30

For the PTW TN23331 (S/N 0833) chamber, the results fluctuated considerably. Especially the point reported by the INER deviated from the others by around 1 %, which was consistent with the instability of the chamber observed in figure 3. These inconsistent results were judged to be due to the instability of the chamber itself.

$R_i$  and  $u_{\text{LINK}}$  were determined as shown in table 8 based on the results of the Exradin A3 (S/N 110) chamber. When  $u_{\text{LINK}}$  was estimated according to equation (7),  $u_{K,\text{LINK},k,\text{stat}}$  and  $u_{I,\text{LINK},k}$  were taken from table 4 and Appendix B, respectively as shown in table 9. Finally, the higher value of  $u_{\text{LINK}}$  (0.36 %) estimated according to equation (10) was applied to equation (4).

It can be seen from Table 8 that in the present comparison the KRISS and NMIJ differ by over 1 %, despite the fact that as seen in Table 4 the two laboratories agree to within 0.1 % in the BIPM.RI(I)-K5 comparison series. Furthermore, a subsequent comparison made in 2018 [15] showed the two laboratories to again agree within 0.1 %. No reason for these differences has been found.

Table 8.  $R_i$  of the participating laboratories

	$R_{i,\text{KRISS}}$	$R_{i,\text{NMIJ}}$	$R_i$	$u_{\text{LINK}} (k = 1)$	
				Acc. to eq. (7)	Acc. to eq. (10)
KRISS	-	0.993 1	0.993 1	0.000 5	-
NMIJ	1.003 3	-	1.003 3	0.000 5	-
INER	0.998 1	0.992 6	0.995 4	0.000 5	0.003 6
CIEMAT	1.007 0	1.001 4	1.004 2	0.000 5	0.003 6
NIM	1.004 1	0.998 5	1.001 3	0.000 5	0.003 6

Table 9. Estimation of  $u_{\text{LINK}} (k = 1)$  according to equation (7)

Uncertainty components	KRISS	NMIJ
$u_{K,\text{LINK},k,\text{stat}}$	0.000 5	0.001 6
$u_{I,\text{LINK},k,\text{stat}}$	(0.000 1)	0.000 1
$u_{I,\text{LINK},k,\text{non-stat}}$	0.000 2	0.000 1
$u_{\text{LINK},k}$	0.000 5 <sup>a)</sup>	0.002 2 <sup>b)</sup>
$u_{\text{LINK}}$	0.000 5	

<sup>a)</sup>  $u_{\text{LINK},\text{KRISS}}$  was calculated according to equation (9).

<sup>b)</sup>  $u_{\text{LINK},\text{NMIJ}}$  was calculated according to equation (8).

The combined standard uncertainties  $u_{R,i}$  are shown in table 10. The physical constants that enter in the air kerma determinations at both the  $i$ -th laboratory and the BIPM were assumed to be fully correlated ( $f_j = 1$ ). Correction factors commonly considered at the  $i$ -th laboratory and the BIPM were assumed to be partially correlated at  $f_j = 0.5$ . The CIEMAT was traceable to the National Physical Laboratory (NPL, United Kingdom). Thus, only the uncertainty components of  $u_i$  related to the physical constants that might have entered in the air kerma determination at the NPL were assumed to be fully correlated, but the rest were assumed to be completely un-correlated.  $u_{\text{BIPM}}$  was 0.19 % as shown in table 4.

Table 10. Estimation of  $u_{R,i}$  ( $k = 1$ ) of the participating laboratories

	$u_i$	$u_{\text{BIPM}}$	$\sqrt{u_i^2 + u_{\text{BIPM}}^2 - \sum_j f_j^2 (u_{i,j}^2 + u_{\text{BIPM},j}^2)}$	$u_{\text{tr}}$	$u_{\text{LINK}}$	$u_{R,i}$
KRISS	0.21	0.19	0.19	0.02	0.36	0.41
NMIJ	0.24	0.19	0.24	0.02	0.36	0.43
INER	0.30	0.19	0.26	0.02	0.36	0.45
CIEMAT	0.78	0.19	0.78	0.02	0.36	0.86
NIM	0.30	0.19	0.25	0.02	0.36	0.44

#### 4. Degrees of equivalence

For the  $i$ -th laboratory having a comparison result  $R_i$  with a combined standard uncertainty  $u_{R,i}$  (as given in Table 10), the degree of equivalence with respect to the reference value was given by a pair of terms [6]:

the relative difference  $D_i$

$$D_i = R_i - 1, \quad (12)$$

and the expanded uncertainty ( $k = 2$ ) of the difference, i.e.

$$U_i = 2u_{R,i}. \quad (13)$$

The values of  $D_i$  for the participating laboratories are summarized in table 11, where  $D_i$  and  $U_i$  are both expressed in mGy/Gy. The largest discrepancy between any of the laboratories and the BIPM was found to be less than 0.5 % and in no case, the degree of equivalence was larger than the expanded uncertainty.

Table 11.  $D_i$  of the participating laboratories

Laboratory $i$	$D_i$	$U_i$
	/ (mGy/Gy)	
INER	-4.6	8.9
CIEMAT	4.2	17
NIM*	1.3	8.8

\* These data are excluded from updating degree of equivalence since this laboratory has participated in a new comparison study (BIPM.RI-K5) [11]

Note that the data of the NIM presented in table 11, while correct at the time of the measurements included in the present report, are out-of-date now because this laboratory has participated in a new comparison (BIPM.RI-K5) [11]. Degree of equivalence of this laboratory in the new comparison is  $(-3.3 \pm 4.2)$ . This is reasonably consistent with  $u_{\text{LINK}}$  (0.36 %) arising from the difference between the two linking laboratories.

Also note that the data presented in table 11 are not adjusted for any subsequent changes to the standards which have been revised at the participating laboratories due to the publication of ICRU report 90 [12]. This is because ICRU report was published in 2016 and the participating laboratories switched to the recommendations of this report in 2018 - 2019. (Please, find the results reflecting the impacts related to ICRU report 90 in Appendix C.)

The validity period of these results is expected to be until 2026. This is because the CCRI made a resolution in which the results from a comparison in the field of radiation dosimetry is valid for 12 years in general (15 years in exceptional cases) from the laboratory completes its measurement [13]. As it is mentioned above, one of the participating laboratories participated in a new comparison study. The remaining two laboratories are suggested to engage in new comparison studies, soon.

The updated results under the CIPM MRA [7] are available in the key comparison database (KCDB) [8].

## 5. Conclusions

A comparison of the air kerma standards for  $^{137}\text{Cs}$  gamma radiation has been carried out among five laboratories. Two transfer chambers were circulated among the five laboratories and each laboratory was asked to report calibration coefficients and the associated uncertainties. The ionization chambers were returned several times to the pilot laboratory during the comparison. One of the ionization chambers showed a significant drift and a sudden change in its response, but the second transfer chamber showed good repeatability. Therefore, the degrees of equivalence of the participating laboratories were evaluated based on the results of the second ionization chamber only.

The results showed the calibration capabilities of all participating laboratories to be in general agreement within the stated uncertainties. As a result, each participating laboratory has not only verified its own measurement capabilities but also strengthened technical cooperation and the exchange of ideas with other laboratories in the process of achieving a comparison result linking it to the BIPM.

The results of this comparison study will be valid until 2026, unless exceptional circumstances arise. This is because the results from a comparison in the field of radiation dosimetry are generally valid for 12 years from the year the laboratory completes its measurement [13]. The usefulness of the comparison results for the participating laboratories has been reduced due to delayed publication of present report. Two laboratories who updated their degree of equivalence through this comparison study are suggested to engage in new comparison studies, soon.

## References

- [1] P.J. Allisy, D.T. Burns and P. Andreo, "International framework of traceability for radiation dosimetry quantities," *Metrologia*, 46, S1-S8 (2009)
- [2] D.T. Burns and D. Butler, "Updated report on the evaluation of degree of equivalence in regional dosimetry comparisons", CCRI(I)/17-09 (2017)
- [3] C. Kessler, P. Roger, P.J. Allisy and C.-Y. Yi, "Comparison of the standards for air kerma of the KRISS and the BIPM for  $^{137}\text{Cs}$  gamma radiation," *Metrologia*, 47, 06022 (2010)
- [4] C. Kessler, N. Saito and T. Kurosawa, "Key comparison BIPM.RI(I)-K5 for the air kerma standards of the NMIJ, Japan and the BIPM in  $^{137}\text{Cs}$  gamma radiation," *Metrologia*, 50, 06022 (2013)
- [5] Evaluation of measurement data – Guide to the expression of uncertainty in measurement, JCGM 100:2008 BIPM, Sèvres, France 2008
- [6] C.M. Sutton, "Analysis and linking of international measurement comparisons," *Metrologia*, 41, 272-277 (2004)
- [7] CIPM MRA: Mutual recognition of national measurement standards and of calibration and measurement certificates issued by national metrology institutes, International Committee for Weights and Measures, 1999, 45 pp. <http://www.bipm.org/pdf/mra.pdf>
- [8] BIPM Key Comparison Database KCDB  $^{137}\text{Cs}$  air kerma comparisons BIPM.RI(I)-K5
- [9] L. Büermann, A.V. Oborin, J. Dobrovosky, V.S. Milevsky, G.W. Salas and A. Lapenas, "COOMET.RI(I)-K1 comparison of national measurement standards of air kerma for  $^{60}\text{Co}$   $\gamma$  radiation," *Metrologia*, 46, Technical Supplement (2009)
- [10] C. Kessler, P.J. Allisy-Roberts and R. Minniti, "Comparison of the standards for air kerma of the NIST and the BIPM for  $^{60}\text{Co}$  gamma radiation," *Metrologia*, 50, 06002 (2013)
- [11] C. Kessler, D.T. Burns, D. Li, and P. Wang, Key comparison BIPM.RI-K5 of the air kerma standards of the NIM, China, and the BIPM in  $^{137}\text{Cs}$  gamma radiation, *Metrologia* 52 (2015) Tech. Suppl. 06009.
- [12] International Commission on Radiation Units and Measurements 2016 Key data for ionizing-radiation dosimetry: measurement standards and applications ICRU Report 90 vol 14 Oxford University Press, 2016.

- [13] Consultative Committee for Ionizing Radiation, Report of the 28th meeting (8-10 June 2021) to the International Committee for Weights and Measures (<https://www.bipm.org/documents/20126/59879237/28th-meeting-2021.pdf/197f08be-1a9e-ab74-29c1-94bf69ee4b52>). .
- [14] D. Burns, and C. Kessler, Re-evaluation of the BIPM international dosimetry standards on adoption of the recommendations of ICRU report 90, Metrologia 55, R21-R26 (2018)
- [15] P. Rindhatayathon, A. Siriwitpreecha, and V. Pungkun, Establishing of primary standard for Cs-137 air-kerma of OAP, Thailand, Applied Radiation and Isotopes 170, 109586 (2021)

## Appendix A

### Instability Issue of the Transfer Ionization Chamber PTW TN23331 (S/N 0833)

Instability issue of transfer ionization chambers used in comparison studies are not usual, but this is not the first time, either. In the case of the COOMET.RI(I)-K1 key comparison of the air kerma for  $^{60}\text{Co}$  gamma radiation performed in 2009, a PTW M23331 ionization chamber produced unstable measurement signals and was not used for the evaluation of the comparison results [9]. Coincidentally, it was the same kind of model that was problematic in this comparison study, only the type of connector was different. Even the fluctuation of the chamber response during the COOMET.RI(I)-K1 key comparison was almost the same as that observed in this study, around 1.3 %. And in the case of the BIPM.RI(I)-K1 key comparison, which was a bilateral comparison study between the National Institute of Standards and Technology and the BIPM, a PTW 30013 chamber showed unstable behavior and was excluded in the final comparison result [10]. This model is usually recognized very stable, but the total drift of the current was 0.17 % over five days.

The KRISS did not manage to figure out what caused the instability of the transfer ionization chamber PTW TN23331 (S/N 0833). On some occasions, the chamber appeared to be stable two hours after the radiation beam was turned on as recommended by the technical protocol, but many times the chamber response continued to drift and the drift did not stop even after the beam was turned off, as shown in the figure A1 (a), (b), (c), (e) and (g). A damage of the chamber's high voltage insulator was suspected to be the cause of the problem, but the leakage current was low at less than 1 fA.

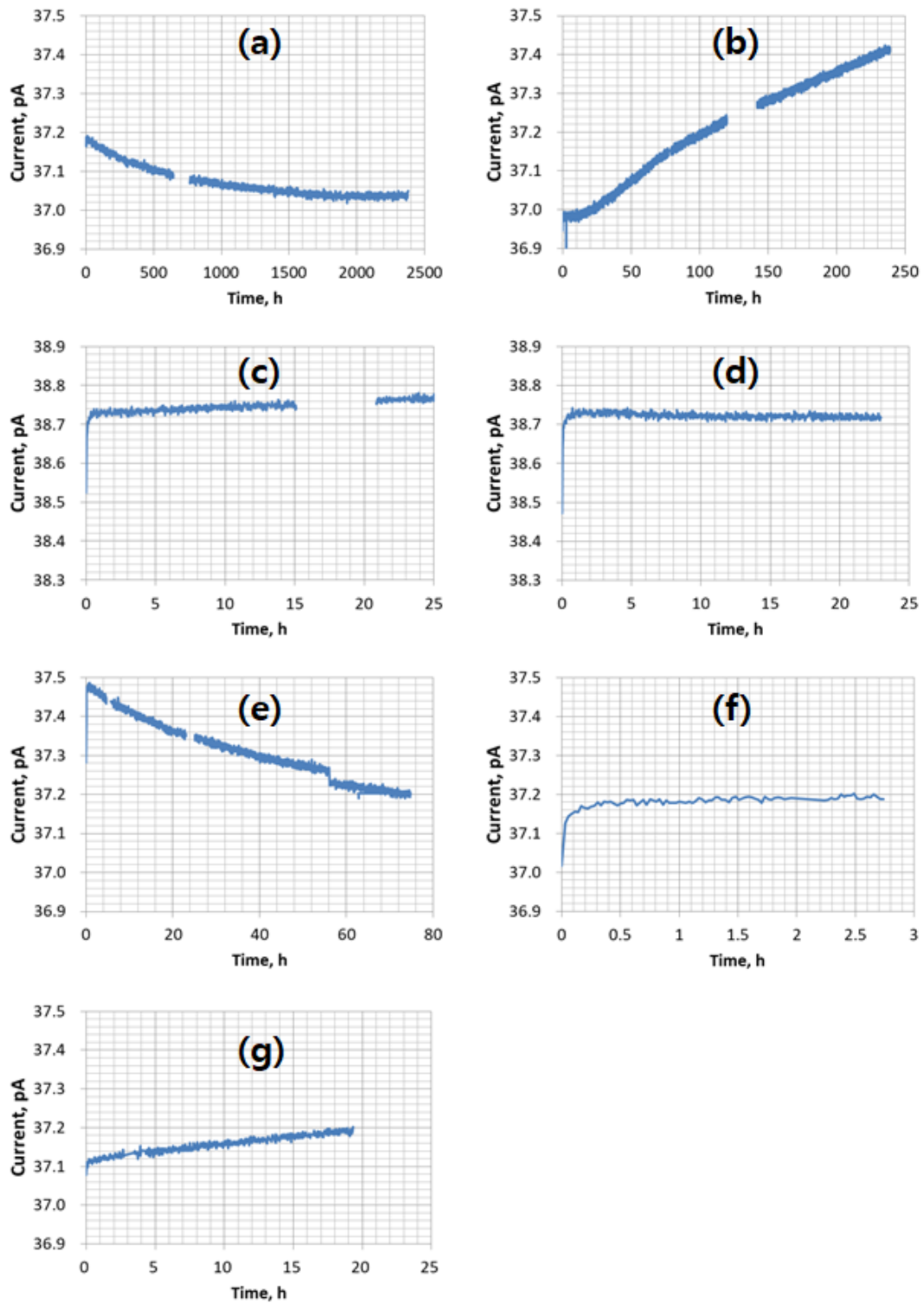


Figure A1. Drift of the ionization current observed with the PTW TN23331 (S/N 0833) chamber as a function of time after the radiation beam was turned on. Measurements (a), (c), (e) and (g) were obtained at 400 V, while measurements (b), (d) and (f) were obtained at -400 V. (a), (b) were obtained from 20-Jan – 3-Feb 2014; (c), (d) from 7-Feb – 9-Feb 2014; (e), (f) from 9-May – 12-May 2014; (g) from 19-Jun -20-Jun 2014.

The chamber was inspected on 10 June 2020 with x-rays using a computer tomography (CT) machine, an Ingenuity TF PET/CT scanner, to find any structural defect on the request of the APMP TCRI in 2019. The CT scanned image around the cavity was as shown in figure A2. The voltage and the current of the CT x-ray tube were tuned to improve the image quality, but only with limited success because the CT machine was not designed to take images of ionization chambers. No damage or defect was found regarding the structure of the chamber. The bright halo around the middle of the image was an artifact caused by the bed on which the chamber was placed.

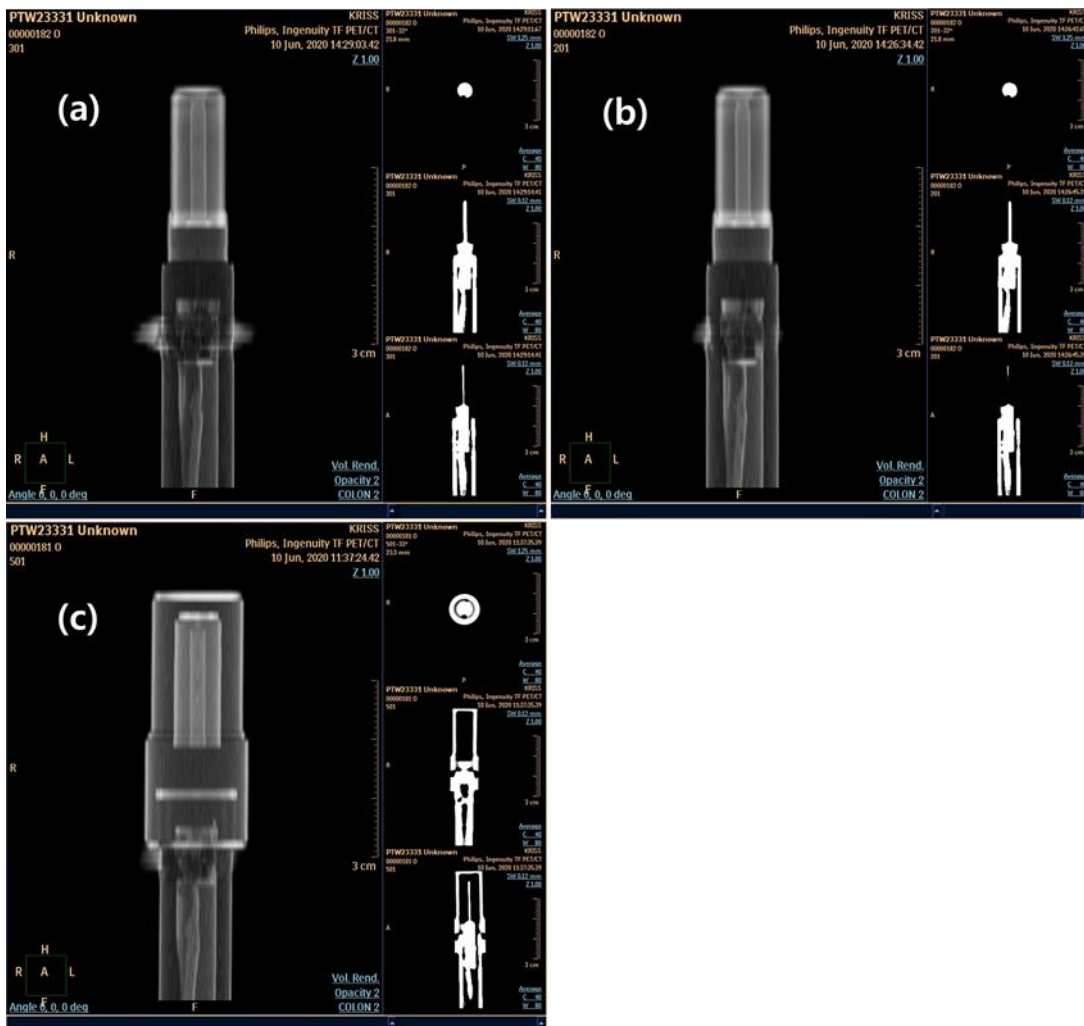


Figure A2. CT scanned image of the PTW TN23331 (S/N 0833) chamber around the cavity area using x-ray beams at 80 kV, 500 mA (a), at 140 kV, 300 mA (b) and at 140 kV, 300 mA with the build-up cap fitted (c).

## Appendix B

### KRISS Uncertainty budget

#### Uncertainty associated with the standard (standard cavity chamber)

Source of component	Relative standard uncertainty (%)	
	Type A	Type B
1. Dry air density		0.01
2. Ratio of mass energy absorption coefficients		0.06
3. Ratio of mass stopping power		0.11
4. Mean energy per charge produced in air		0.00
5. Energy loss to bremsstrahlung		0.00
6. Correction factors		
Humidity	0.00	0.03
Recombination	0.01	0.02
Stem scattering	0.04	
Chamber wall attenuation		0.03
Chamber wall scattering	0.01	0.03
Insulator compound	0.01	0.11
Reabsorption of bremsstrahlung	0.00	0.01
Axial non-uniformity	0.01	0.05
Radial non-uniformity	0.01	0.02
Radioactive decay	0.00	0.00
Other corrections if any		
7. Ionization current	0.01	0.02
8. Chamber volume	0.00	0.05
<b>Quadratic sum</b>	0.05	0.19
<b>Combined standard uncertainty</b>		0.20

#### Uncertainty associated with the calibration of the transfer chambers

Source of component	Relative standard uncertainty (%)	
	Type A	Type B
1. Reference air kerma rate		0.20
2. Ionization current	0.01	0.02
3. Correction factors		
Air density correction (pressure & temperature)		0.02
Humidity		0.03
Transfer chamber positioning		
4. Other correction factors (if any)		
Thermal expansion		0.01
Decay correction		0.00
<b>Quadratic sum</b>	0.01	0.21
<b>Combined standard uncertainty</b>		0.21

## NMIJ Uncertainty budget

### Uncertainty associated with the standard (standard cavity chamber)

Source of component	Relative standard uncertainty (%)	
	Type A	Type B
1. Dry air density		0.01
2. Ratio of mass energy absorption coefficients		0.05
3. Ratio of mass stopping power		0.11
4. Mean energy per charge produced in air		0.02
5. Energy loss to bremsstrahlung		0.02
6. Correction factors		
Humidity		0.02
Recombination		0.01
Stem scattering	0.01	0.10
Chamber wall attenuation		0.10
Chamber wall scattering	0.05	0.10
Insulator compound		
Reabsorption of bremsstrahlung		
Axial non-uniformity		0.10
Radial non-uniformity		
Radioactive decay		
Scattering photon effect (mass-energy absorption coefficient ratio, stopping power ratio and wall correction factor)		0.06
Environmental condition under which the measurement is done (temperature and pressure)		0.03
position of the primary chamber		0.04
7. Ionization current	0.01	0.01
8. Chamber volume	0.01	0.01
<b>Quadratic sum</b>	0.05	0.23
<b>Combined standard uncertainty</b>		0.23

### Uncertainty associated with the calibration of the transfer chambers

Source of component	Relative standard uncertainty (%)	
	Type A	Type B
1. Reference air kerma rate	0.05	0.23
2. Ionization current	0.03	0.01
3. Correction factors		
Air density correction (pressure & temperature)		0.03
Humidity		0.02
Transfer chamber positioning		0.04
4. Other correction factors (if any)		
<b>Quadratic sum</b>	0.06	0.24
<b>Combined standard uncertainty</b>		0.24

## INER Uncertainty budget

### Uncertainty associated with the standard (standard cavity chamber)

Source of component	Relative standard uncertainty (%)	
	Type A	Type B
1. Dry air density		0.01
2. Ratio of mass energy absorption coefficients		0.05
3. Ratio of mass stopping power		0.11
4. Mean energy per charge produced in air		0.02
5. Energy loss to bremsstrahlung		0.02
6. Correction factors		
Humidity		0.03
Recombination	0.01	
Stem scattering	0.03	
Chamber wall attenuation		0.08
Chamber wall scattering		
Insulator compound		
Reabsorption of bremsstrahlung		
Axial non-uniformity	0.10	
Radial non-uniformity	0.10	
Radioactive decay		0.01
Atmospheric pressure & temperature correction		0.03
Primary chamber positioning		0.06
7. Ionization current	0.04	0.03
8. Chamber volume		0.05
<b>Quadratic sum</b>	<b>0.15</b>	<b>0.17</b>
<b>Combined standard uncertainty</b>		<b>0.23</b>

### Uncertainty associated with the calibration of the transfer chambers

Source of component	Relative standard uncertainty (%)	
	Type A	Type B
1. Reference air kerma rate	0.15	0.17
2. Ionization current	0.15	0.03
3. Correction factors		
Air density correction (pressure & temperature)		0.03
Transfer chamber positioning		0.11
<b>Quadratic sum</b>	<b>0.21</b>	<b>0.21</b>
<b>Combined standard uncertainty</b>		<b>0.30</b>

## **CIEMAT Uncertainty budget**

### **Uncertainty associated with the calibration of the transfer chambers**

<b>Source of component</b>	<b>Relative standard uncertainty (%)</b>	
	<b>Type A</b>	<b>Type B</b>
1. Reference air kerma rate	0.07	0.76
2. Ionization current	0.02	0.06
3. Correction factors		
Air density correction (pressure & temperature)		0.05
Humidity		0.03
Transfer chamber positioning		0.12
4. Other correction factors (if any)		
<b>Quadratic sum</b>	0.07	0.77
<b>Combined standard uncertainty</b>		0.78

## NIM Uncertainty budget

### Uncertainty associated with the standard (standard cavity chamber)

Source of component	Relative standard uncertainty (%)	
	Type A	Type B
1. Dry air density		0.01
2. Ratio of mass energy absorption coefficients		0.05
3. Ratio of mass stopping power		0.11
4. Mean energy per charge produced in air		0.02
5. Energy loss to bremsstrahlung		0.02
6. Correction factors		
Humidity		0.03
Recombination	0.06	0.05
Stem scattering	0.04	
Chamber wall attenuation		0.10
Chamber wall scattering	0.04	
Insulator compound		
Reabsorption of bremsstrahlung		
Axial non-uniformity	0.05	0.06
Radial non-uniformity	0.05	0.08
Radioactive decay		
Other corrections if any		
7. Ionization current	0.04	0.03
8. Chamber volume		0.09
<b>Quadratic sum</b>	0.12	0.22
<b>Combined standard uncertainty</b>		0.25

### Uncertainty associated with the calibration of the transfer chambers

Source of component	Relative standard uncertainty (%)	
	Type A	Type B
1. Reference air kerma rate	0.12	0.22
2. Ionization current	0.06	0.05
3. Correction factors		
Air density correction (pressure & temperature)	0.03	0.05
Humidity		0.03
Transfer chamber positioning	0.04	0.03
4. Other correction factors (if any)		
Beam non-uniformity		0.10
Repeatability	0.08	
<b>Quadratic sum</b>	0.16	0.26
<b>Combined standard uncertainty</b>		0.30

## Appendix C

### Revised results reflecting the impact of ICRU report 90

This appendix presents revised data of the participating laboratories reflecting the impact of ICRU report 90 [12].

Participating laboratories has submitted to the pilot laboratory the ratio  $R_K$  which is given as

$$R_K = \frac{K_{\text{ICRU 90}}}{K_{\text{old}}} \quad (\text{C.1})$$

where  $K_{\text{ICRU 90}}$  and  $K_{\text{old}}$  respectively are the revised and old air kerma standard of the participating laboratory. Reported  $R_K$  and the relative standard uncertainty of the air kerma standard of the laboratories are as shown in table C1. Uncertainty of the air kerma standard has commonly increased due to the increased uncertainty of  $W_{\text{air } S_{\text{g,air}}}$  in ICRU report 90.

Table C1. Ratio of the revised air kerma standard ( $K_{\text{ICRU 90}}$ ) to the old ( $K_{\text{old}}$ )

	$R_K$	$u_K (k = 1)$	
		$K_{\text{ICRU 90}}$	$K_{\text{old}}$
KRISS	0.993 1	0.39 %	0.20 %
NMIJ	0.991 9	0.41 %	0.23 %
INER	0.993 2	0.24 %	0.18 %
CIEMAT	0.990 0	0.85 %	0.75 %
NIM	0.992 0	0.27 %	0.25 %
BIPM [14]	0.991 9	0.19 %	0.19 %

$R_{\text{LINK,BIPM}}$  of a linking laboratory defined by equation (2) is re-evaluated as

$$R_{\text{LINK,BIPM}}^{\text{ICRU90}} = R_{\text{LINK,BIPM}} \frac{R_{\text{K,LINK}}}{R_{\text{K,BIPM}}} \quad (\text{C.2})$$

where  $R_{\text{K,LINK}}$  and  $R_{\text{K,BIPM}}$  are the ratio  $R_K$  of the linking laboratory and the BIPM.  $R_{\text{K,BIPM}}$  is given in table C.1. Table C2 shows calculation results of  $R_{\text{LINK,BIPM}}^{\text{ICRU90}}$  of the linking laboratories. In table C2, the related uncertainties are also revised.

Table C2.  $R_{\text{LINK,BIPM}}^{\text{ICRU90}}$  of the LINKs in the key comparison study of the air kerma for  $^{137}\text{Cs}$  gamma-rays, BIPM.RI(I)-K5

	$R_{\text{LINK,BIPM}}$	$R_{\text{LINK,BIPM}}^{\text{ICRU90}}$	Relative standard uncertainties, %			
			$u_{\text{K,LINK,stat}}$	$u_{\text{K,LINK,non-stat}}$	$u_{\text{I,LINK,stat}}$	$u_{\text{I,LINK,non-stat}}$
KRISS	0.998 6	0.999 8	0.05	0.35	0.01	0.02
NMIJ	0.997 7	0.997 7	0.16	0.39	0.01	0.01

$R_i$  of a participating laboratory defined by equation (1) is re-evaluated as

$$R_i^{\text{ICRU90}} = R_i \frac{R_{\text{K},i}}{R_{\text{K,BIPM}}}. \quad (\text{C.3})$$

$R_i^{\text{ICRU90}}$  and  $u_{\text{LINK}}$  are determined as shown in table C3.  $u_{\text{LINK}}$  estimated according to either of equation (7) or (10) did not change.

Table C3.  $R_i^{\text{ICRU90}}$  of the participating laboratories

	$R_{i,\text{KRISS}}^{\text{ICRU90}}$	$R_{i,\text{NMIJ}}^{\text{ICRU90}}$	$R_i^{\text{ICRU90}}$	$u_{\text{LINK}} (k = 1)$	
				Acc. to eq. (7)	Acc. to eq. (10)
KRISS	-	0.994 3	0.994 3	0.000 5	-
NMIJ	1.003 3	-	1.003 3	0.000 5	-
INER	0.999 4	0.993 9	0.996 7	0.000 5	0.003 6
CIEMAT	1.005 1	0.999 5	1.002 3	0.000 5	0.003 6
NIM	1.004 2	0.998 6	1.001 4	0.000 5	0.003 6

The combined standard uncertainties  $u_{R,i}$  are estimated as shown in table C4. The increase of  $u_{\text{K}}$  shown in table C1 has been accounted for in the estimation of  $u_i$ . The physical constants that enter in the air kerma determinations at both the  $i$ -th laboratory and the BIPM are assumed to be fully correlated ( $f_j = 1$ ) as they were in table 10 including  $W_{\text{air}, S_{\text{g,air}}}$ .

Table C4. Estimation of  $u_{R,i} (k = 1)$  of the participating laboratories

	$u_i$	$u_{\text{BIPM}}$	$\sqrt{u_i^2 + u_{\text{BIPM}}^2 - \sum_j f_j^2 (u_{i,j}^2 + u_{\text{BIPM},j}^2)}$	$u_{\text{tr}}$	$u_{\text{LINK}}$	$u_{R,i}$
KRISS	0.39	0.19	0.30	0.02	0.36	0.47
NMIJ	0.41	0.19	0.34	0.02	0.36	0.49
INER	0.34	0.19	0.35	0.02	0.36	0.50
CIEMAT	0.87	0.19	0.87	0.02	0.36	0.94
NIM	0.33	0.19	0.26	0.02	0.36	0.44

The values of  $D_i^{\text{ICRU90}}$  for the participating laboratories are summarized in table C5, where  $D_i^{\text{ICRU90}}$  and  $U_i$  are both expressed in mGy/Gy. Change in the degree of equivalence is small since the impact of ICRU report 90 was globally common. However, uncertainty has increased due to the increased uncertainty of  $W_{\text{air}, s_{\text{g,air}}}$  in ICRU report 90. The degrees of equivalence of the participating laboratories are still lower than the involved expanded uncertainties.

Table C5.  $D_i^{\text{ICRU90}}$  of the participating laboratories

Laboratory $i$	$D_i^{\text{ICRU90}}$	$U_i^{\text{ICRU90}}$
	/ (mGy/Gy)	
INER	-3.3	10
CIEMAT	2.3	19
NIM*	1.4	8.9

\* Note that this laboratory has participated in a new comparison study (BIPM.RI-K5) [11]